Molecular-beam study of sticking of oxygen on Si(100)

T. Miyake, S. Soeki, H. Kato, T. Nakamura, and A. Namiki
Toyohashi University of Technology, Toyohashi 441, Japan

H. Kamba and T. Suzaki
Toyoko Kagaku Co. Ltd., Kawasaki 221, Japan

(Received 7 May 1990; revised manuscript received 31 July 1990)

Molecular-beam techniques have been used to probe the sticking dynamics of molecular oxygen on Si(100) surfaces. The initial sticking probability S_0 is measured with Auger-electron spectroscopy as a function of surface temperature T_s for various incident energies E_i. At $E_i=0.09$ eV, where the trapping-desorption process is dominant, S_0 *decreases* with increasing T_s. This fact indicates that sticking is predominantly a physisorption-mediated process. On the other hand, at $E_i=0.9$ eV, S_0 *increases* with increasing T_s. Since the direct inelastic-scattering process is dominant at this energy, this fact suggests that sticking occurs via direct access to molecular chemisorption which will successively go on to dissociative adsorption. Finally, we discuss a mechanism of sticking in terms of an electron transfer from Si to the incident O_2.

I. INTRODUCTION

Dissociative adsorption of molecular oxygen O_2 on Si surfaces, so-called sticking, is now of considerable interest and importance in understanding the early stages of Si oxidation. In the last decade, the process of dissociative adsorption of O_2 on Si has been studied by static methods[1-7] at low surface temperatures T_s, while dynamical processes of sticking have been less studied.[8-10] Schell-Sorokin and Demuth[1] proposed that dissociative adsorption proceeds via a physisorbed molecular state, because in the electron-energy-loss-spectroscopy (EELS) measurement on Si(111) surface at 20 K, physisorbed O_2 was observed simultaneously with dissociated oxygen atoms. The physisorbed state disappeared at 65 K. The buildup of the dissociative adsorptions even at 20 K seems to indicate that the potential barrier of the precursor for dissociation is very small. On the other hand, chemisorbed O_2 has been proposed as precursor to dissociation above 100 K by several other groups.[2-4,7] Ibach, Bruchmann, and Wagner[2] first observed chemisorbed O_2 on Si(111) and Si(100) surfaces at $T_s=100$ and 300 K by EELS measurements. They interpreted it as the peroxy radical theoretically proposed by Goddard *et al.*[11] Edamoto *et al.*[3] also recognized very small amounts of the same band at 300 K on Si(111), and postulated approximately one electron-transferred state, or monovalent anion for chemisorbed O_2. Umbach and his collaborators[4] observed slowly decaying molecular species on Si(111) at 150 and 300 K in the O(1*s*) x-ray photoemission spectra. As a metastable precursor to stable dissociated adsorption, a perioxide bridge configuration was considered. Silvestre and Shayegan[7] estimated 40 ± 15 meV activation energy for the conversion from such precursor to dissociation on Si(111) in their work-function measurement.

Quite few dynamical approaches to the understanding of dissociative absorption of O_2 on Si(100) have been made with a molecular-beam technique.[8-10] Yu and Eldridge[8] measured kinetic processes of the reaction of O_2 followed by vaporization of SiO at high T_s above 800 °C using short pulses (17 μs) of O_2 beams. They found that the O_2 reaction (dissociative adsorption) probabilities with Si(100) at $T_s=950$ °C increased from 0.01 to 0.4 when the normal energies, E_n, of the total incident energies E_i (with $E_n=E_i\cos^2\theta_i$) were increased from 0.01 to 1.0 eV. On the other hand, D'Evelyn, Nelson, and Engel[9] measured initial sticking probability S_0 of Si(100) as a function of T_s for various E_i ranging from 0.1 to 0.6 eV at an incident angle $\theta_i=75°$ (thence $E_n<0.04$ eV). They found two different channels to dissociative adsorption characterized by T_s rather than by E_i or E_n: For $T_s<500-600$ K, S_0 decreased with increasing T_s, whereas for $T_s>600$ K, S_0 increased with increasing T_s. They postulated that at low T_s the dissociative adsorption is mediated by the physisorption of O_2, while at high T_s a direct dissociative adsorption proceeds without passing through any precursor state. However, because of the limited time resolution in their detection systems, neither the O_2 desorption from the physisorption wells nor the direct inelastic scattering were directly detected. The chemisorbed O_2, which has been studied with static methods mentioned above, was not involved as possible precursors to dissociation because it was thought that electron spectroscopic evidence for such chemisorbed molecular species was less convincing on Si(100).

Two scattering processes, trapping desorption and direct inelastic scattering, have been well established in beam experiments[12] for various combinations of incident atoms or molecules and surfaces. Trapping desorption takes place at lower E_i, while direct inelastic scattering predominantly occurs at higher E_i. Simultaneous measurements of scattering and sticking are expected to reveal the expected two channels to dissociative adsorption of O_2 on Si: the physisorption-mediated channel and the direct channel. In this work S_0 is measured as a function

of T_s for various E_i, and trapping probabilities are measured simultaneously. The trapping desorption predominantly occurs at $E_i=0.09$ eV, where S_0 is found to decrease with increasing T_s, whereas the direct inelastic scattering predominantly occurs at $E_i=0.9$ eV, where S_0 is found to increase with increasing T_s. Thus sticking at high E_i proceeds via another channel without physisorption. Finally, we discuss the mechanism of dissociative adsorption in terms of electron transfer from Si to the incident O_2, namely an intermediate negative-ion state, for both channels.

II. EXPERIMENT

E_i of the O_2 beam was varied from 0.09 to 0.9 eV by seeding O_2 into He at a 1:10 ratio through a heatable quartz nozzle with a diameter of 0.05 mm. The O_2 beams were skimmed, chopped, and directed into the main chamber. The O_2 beams at the sample position had a diameter of 1.7 mm and the pulse width was 15 μs. The base pressure of the main chamber was $(6-8)\times10^{-11}$ Torr and it increased to 3×10^{-10} Torr when the beam was introduced. The chamber is equipped with two quadrupole mass spectrometers ($QMS_{1,2}$); the QMS_1 is used for monitoring incident beams and also the partial pressures of O_2 in order to obtain a relative flux of the beam, and the QMS_2 is utilized for detecting scattered O_2. The flight distance between the sample and an ionizing volume of the QMS_2 is 95 mm.

The oxygen coverage Θ after O_2 beam irradiation was measured by Auger-electron spectroscopy at the center of the beam spot on Si surfaces. For the thin oxide layer below 1 monolayer (ML; 1 ML$\equiv6.78\times10^{14}$ cm^{-2}) coverage, oxygen coverage is proportional to the Auger intensity ratio of $I(\mathrm{O}(KLL))/I(\mathrm{Si}(LVV))$. 1 ML oxygen coverage was determined referencing an $I(\mathrm{O}(KLL))/I(\mathrm{Si}(LVV))$ intensity ratio measured at 20 L (1 L$=1\times10^{-6}$ Torr s) background O_2 exposures through a variable leak valve, where the rapid oxygen uptake becomes dull at 1 ML coverage.[2] This was based on the experimental fact that the oxygen uptake curve plotted as $I(\mathrm{O}(KLL))/I(\mathrm{Si}(LVV))$ intensity ratios with background O_2 gas was quite similar to the $I(\mathrm{O}(KLL))/I(\mathrm{Si}(LVV))$ intensity ratios obtained by Ibach *et al.*[2]

Time-of-flight (TOF) distributions and angular distributions of scattered O_2 from Si(100) surfaces were measured by the QMS_2. The angular distributions were obtained by rotating the sample around a rotational axis with fixed angles of 60° between the incident beam and the QMS_2. Rotating the sample instead of rotating QMS_2 may result in inevitable changes of angular resolutions and also in changes of E_n from point to point in angular scans. Since the flight distance is larger than the 1.7 mm beam diameter at the surface for $\theta_i=0°$ incidence, the angular resolutions are approximately fixed over the angles from $\theta_i=-15°-60°$. If the scattering of O_2 is dominated by the trapping-desorption process, the TOF distribution will be generally fitted to a single Maxwell-Boltzmann distribution whose temperature is approximately equal to T_s, and the angular distribution will obey a cosine distribution. Therefore, a deviation from the cosine distribution may be due to the direct inelastic-scattering process.[12] Because of certain ambiguities inherent to the sample rotation for the angular scans, we will have to be satisfied with deduction of qualitative trapping probabilities from the angular distributions.

The samples used in the present experiment were Si(100) wafers (p type, 10 Ω cm) with 15 mm$\times$17 mm rectangles. The Si(100) surfaces were pretreated by chemical etching in hydrogen fluoride solutions and were subsequently oxidized in HCl-H_2O_2 solutions to protect the surfaces against carbon contamination. The sample was flashed to 1100 K in the UHV chamber to remove the oxide layer. Ar^+ sputtering (incident angle θ_i of 70° from the surface normal, 2 μA, 4 kV) followed by annealing at 1100 K were generally sufficient to produce clean surfaces with a C((KLL)) to Si((LVV)) ratio of less than 0.01. The samples were always flashed out to ensure a clean surface prior to each observation. T_s was controlled by direct Ohmic heating through the samples and monitored by a Chromel-Alumel thermocouple and also by an infrared pyrometer. Other experimental details have been reported elsewhere.[13]

III. RESULTS AND DISCUSSION

Sticking kinetics of O_2 on the Si(100) surface are determined from the oxygen coverage versus O_2 irradiation curves, which were measured systematically as a function of T_s over the range from 300 to 900 K and as a function of E_i ranging from 0.09 to 0.9 eV. Examples of such curves at $T_s=300$ K are shown in Fig. 1. It is apparent that the sticking probabilities S ($S=d\Theta/2\times\mathrm{flux}\times dt$) decreased with increasing Θ. The initial sticking probability S_0 (corresponding to dissociative adsorption on the

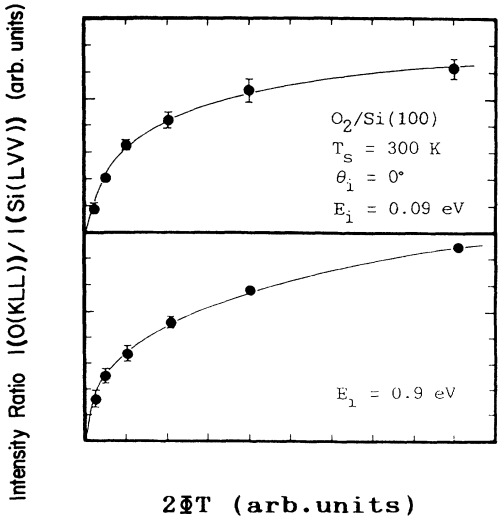

FIG. 1. Ratios of $I(\mathrm{O}(KLL))$ to $I(\mathrm{Si}(LVV))$ vs O_2 beam exposure ($2\Phi T$) curves, where Φ is the incident-beam flux and T is the accumulated exposure time. 1 monolayer oxygen coverage was determined referencing the $I(\mathrm{O}(KLL))/I(\mathrm{Si}(LVV))$ intensity ratio at 20 L background O_2 exposures.

clean surface above 300 K), was determined from the initial slope of the oxygen coverage versus O_2 beam exposure curves. Because of the lack of the absolute beam flux, S_0 cannot be determined absolutely, and relative values are obtained. Rather scattered S_0 values have been reported ranging from 2×10^{-4} to 0.2 at $T_s=300$ K in static measurements,[14] while $S_0=0.01$ was reported in beam measurements at $T_s=300$ K.[9]

The T_s dependence of S_0 for $E_i=0.09$, 0.3, and 0.9 eV shows quite an interesting feature as demonstrated in Fig. 2. For $E_i=0.09$ eV, S_0 decreased with increasing T_s for the entire range from $T_s=300$ to 900 K. For $E_i=0.3$ eV, S_0 are found to be approximately constant or slightly increased. On the other hand, for $E_i=0.9$ eV, S_0 increased quite sharply with increasing T_s. An apparent decrease in S_0 was obtained above 800 K, which was due to SiO desorption.[8-10] At $E_i=0.9$ eV and $\theta_i=71°$, S_0 was found to be smaller than S_0 at $\theta_i=0°$, suggesting that S_0 cannot be simply scaled by either E_i or E_n. The overall trend of S_0, observed in Fig. 2, seems to be somewhat different from the original plots of S_0 versus T_s curves by D'Evelyn, Nelson, and Engel.[9] They observed a minimum S_0 around $T_s=500$–600 K for the tested energy range E_i from 0.08 to 0.6 eV. Our curves for $E_i=0.09$ and 0.3 eV in Fig. 2 appear to be similar to the curves obtained by Engstrom and Engel[10] after replotting their original data. These different T_s dependences of S_0 curves seem to indicate that different mechanisms are operative depending on E_i for dissociative adsorption between 0.09 and 0.9 eV. Here we consider that sticking at $E_i=0.09$ eV proceeds via physisorption followed by subsequent chemisorption of O_2 at any T_s, whereas sticking for $E_i=0.9$ eV proceeds via direct access to chemisorbed O_2. Hereafter, the former sticking is called physisorption-chemisorption-mediated sticking, or PC sticking, and the latter is called direct chemisorption-mediated sticking, or DC sticking. For $E_i=0.3$ eV, the behavior of S_0 is a mixed process of both PC and DC stickings. These two T_s dependent channels of sticking are directly confirmed by measurements of the scattering process as follows.

The angle-resolved TOF spectra of scattered O_2 were measured over a wide range of conditions of T_s and E_i. Figure 3 shows one example of TOF spectra obtained at $T_s=300$ K, $\theta_i=30°$, and $\theta_r=30°$. The upper spectrum

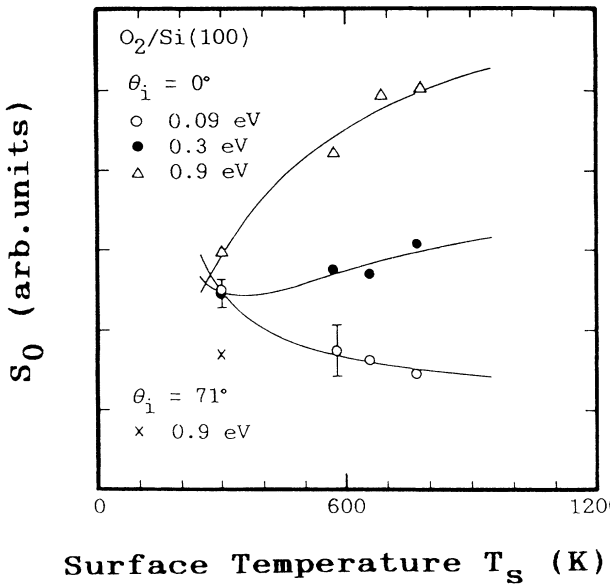

FIG. 2. Initial sticking probability S_0 vs surface temperature T_s for the three different beam energies. The solid lines are obtained by a least-squares fit to Eq. (2).

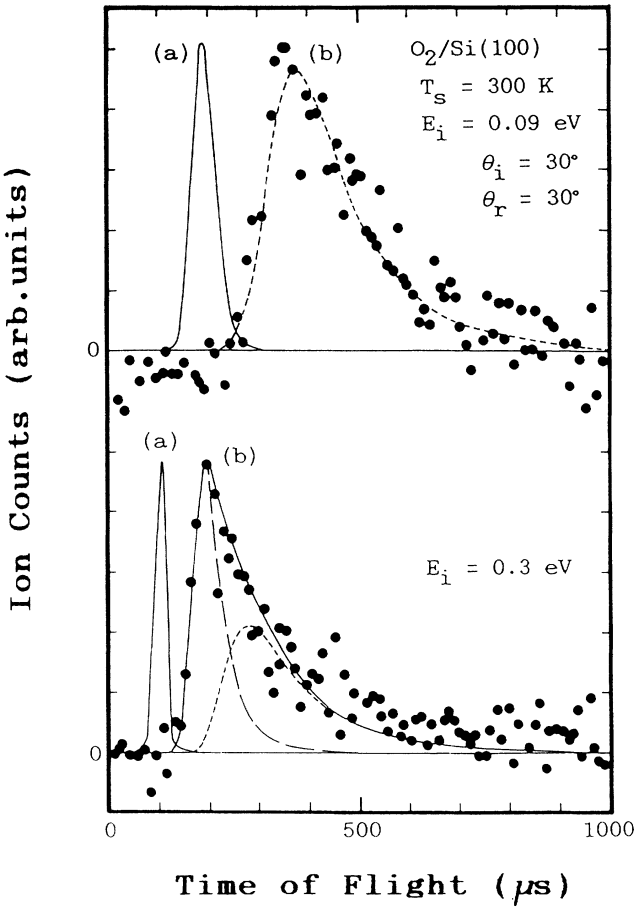

FIG. 3. Time-of-flight distributions for scattered O_2 from Si(100) at $T_s=300$ K. (a) Time profiles of the incident beams; (b) time-of-flight distributions of scattered O_2. The short-dashed curves display a Maxwell-Boltzmann distribution characterized with T_s for the trapping-desorption component. The TOF curve, which obeys the Maxwell distribution, can be given by $L_{td}(t)=A_{td}/t^4\exp[-(m/2kT_s)(L/t)^2]$, where L is a flight distance. The long-dashed curves display a shifted Maxwell-Boltzmann distribution for the direct inelastic-scattering component, which is given by $I_{di}(t)=A_{di}/t^4\exp[-(m/2kT_{di})(L/t-v_0)^2]$. The curve for $E_i=0.3$ eV in Fig. 3 shows the best-fit curve for $I(t)=I_{td}(t)+I_{di}(t)$ for the parameters, $T_{di}=331$ K, $L=0.095m$, $v_0=648m/s$, $A_{de}=0.43$, and $A_{di}=0.97$. Here, each curve has been convoluted with the incident-beam profile.

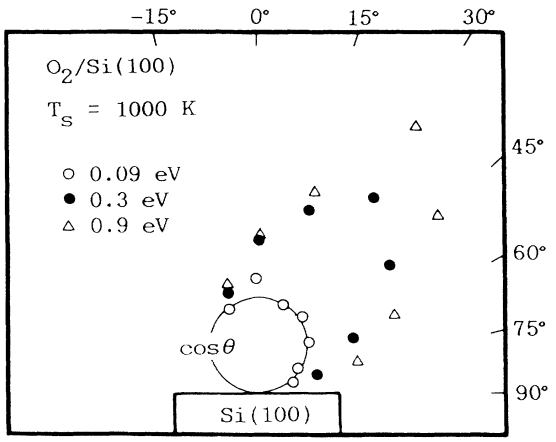

FIG. 4. Angular distributions for scattered O_2 from Si(100) at $T_s=1000$ K. Each point is an accumulated intensity of the TOF distribution of scattered O_2, and its intensity is normalized to the cosine component for each E_i. The cosine part for each E_i has been referenced with the ratio of the direct inelastic component to the trapping-desorption component in the respective TOF spectrum obtained at $\theta_i=0°$.

was obtained for $E_i=0.09$ eV, and the lower one for $E_i=0.3$ eV. The solid curves (a) show time profiles of the incident beams at the sample. The short-dashed curves display a Maxwell-Boltzmann distribution characterized by a T_s for trapping desorption. The long-dashed curves indicate a shifted Maxwell-Boltzmann distribution for direct inelastic scattering. For $E_i=0.09$ eV, it is clear that TOF distribution of scattered O_2 comprises only one component, which can be fitted with the Maxwell-Boltzmann distribution characterized by T_s. Therefore, the scattering of O_2 is dominated by the trapping-desorption process at $E_i=0.09$ eV. On the other hand, at $E_i \gtrsim 0.3$ eV, TOF spectra of the scattered O_2 are clearly bimodal, suggesting that both trapping-desorption and direct inelastic-scattering processes take place.

Figure 4 shows the angular distributions of O_2 scattering at $T_s=1000$ K. For $E_i=0.09$ eV, the angular distribution is almost cosine at $T_s=300-1000$ K, while for $E_i \gtrsim 0.3$ eV, the distributions show a clear deviation from a cosine distribution to a lobular pattern in the specular direction. This result confirms again that the O_2 scattering is dominated by the trapping-desorption process at $E_i=0.09$ eV. On the other hand, the lobular pattern towards specular angles indicates that the direct inelastic-scattering process is involved in the O_2 scattering for $E_i \gtrsim 0.3$ eV. The deviation from the cosine increases with increasing E_i. This means that direct inelastic scattering becomes dominant for larger E_i. For a tentative evaluation of trapping probability from Fig. 4, we changed the scattered intensities to the flux values, because the values in Fig. 4 were measured as a density rather than a flux, and we assumed that the flux of the direct inelastic component of the out-of-plane scattering is half the intensities of the in-plane scattering, following Kuipers *et al.*[15] Here, the $\cos\theta$ curve is normalized by the ratio of the trapping-desorption component to the direct inelastic-scattering component in the TOF spectra at $\theta_i=0°$. As a result, P_{trap} at $T_s=1000$ K were estimated to be 0.98 (0.97), 0.71 (0.71), and 0.11 (0.02) at $E_i=0.09$, 0.3, and 0.9 eV, respectively, where the values in parentheses are P_{trap} at 300 K. The values estimated in this way should be considered to be showing only a qualitative measure for the trapping probability because of inevitable error in the polar plots of the scattered yield arising from sample rotation instead of the detector. Qualitatively speaking, for $E_i=0.09$ eV, the trapping probability is very large, while for $E_i=0.9$ eV, it is extremely small. For $E_i=0.3$ eV, the trapping probability seems to be somewhat small compared with $E_i=0.09$ eV. The temperature effect of the trapping probability is small. These features are well compatible with the TOF spectra obtained for the corresponding E_i.

Therefore, from the results of TOF and angular distributions, we conclude that the scattering of O_2 at $E_i=0.9$ eV is dominated by direct inelastic scattering, whereas at $E_i=0.09$ eV, trapping desorption dominates. Then, it is quite clear that sticking at $E_i=0.09$ keV, where S_0 is characterized as a decreasing function with increasing T_s as shown in Fig. 2, occurs via physisorption. On the other hand, sticking at $E_i=0.9$ eV, where S_0 is characterized by an increasing function with increasing T_s, occurs rather directly, i.e., sticking proceeds in a single collision process with the surface, competing with both the direct inelastic scattering and the trapping into the physisorption well.

For a mechanism of O_2 sticking on Si, we invoke a short-lived O_2^- state as an intermediate precursor just before completing the dissociation of O_2. This is based on static investigations of chemisorbed molecular oxygen,[2-4] as reviewed in the Introduction, e.g., a peroxy radical or a peroxide bridge which was assigned to be approximately one electron-transferred state.[3] For such O_2^- intermediates, we have to note that alkali-metal atoms on Si can enhance sticking probability very dramatically[16-19] by a factor of 10^4-10^5. For this enhancement in S_0, O_2^- formation was suggested to play a key role.[18] The lowering of surface work functions due to metal-atom depositions may make the electron transfer from the surface to the incident O_2 easier, as compared when the surface is clean. Quite recently, O_2^- was directly detected in the grazing incident O_2^+ ion beam scattering from Si(100).[20] This fact strongly suggests that O_2^- is a possible precursor for dissociation. In addition to these facts on Si surfaces, such a negative-ion state has recently been invoked in studies on metal surfaces to explain the dissociative adsorption of O_2 on Pt (Ref. 21) and Ag (Ref. 22), O_2^- evolution in O_2^+ scattering from Ag,[23] and the vibrational excitations of scattered NO from Ag.[24] Holloway and Gadzuk[25] theoretically gave a general basis of the role of intermediate negative-ion states as channels for both dissociative adsorption and vibrational excitations of scattered molecules using the trajectory theory for the relevant potential-energy surfaces.

A kinetic scheme of dissociative adsorption of O_2 on Si(100) may thus be described as follows:

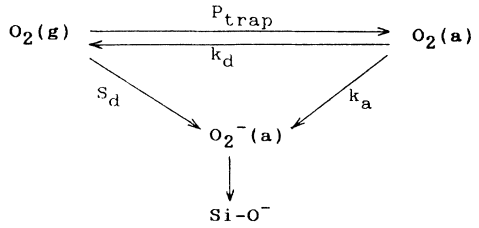

(1)

where $O_2(g)$, $O_2(a)$, and Si-O^- refer to the gas phase O_2, physisorbed O_2, and dissociatively chemisorbed species, respectively. The DC sticking follows the channel, $O_2(g) \rightarrow O_2^-(a) \rightarrow$ Si-O^-, assuming the rapid conversion of $O_2^-(a)$ to Si-O^- at $T_s \gtrsim 300$ K and at clean surfaces, and PC sticking follows the channel, $O_2(g) \rightarrow O_2(a) \rightarrow O_2^-(a) \rightarrow$ Si-O^-; S_d is the DC sticking probability, k_d the rate of desorption, and k_a the rate of dissociative adsorption from relaxed $O_2(a)$. Once the resonantly prepared O_2^- state has been relaxed to $O_2^-(a)$ at the surface, the reverse transitions from $O_2^-(a)$ to $O_2(a)$ or to $O_2(g)$ may be small due to the large activation energy, while dissociation of $O_2^-(a)$ to Si-O^- may be fast, taking into account dissociative adsorption even at 20 K.[1] Assuming Arrhenius forms for the relevant rate constants and also for S_d, $S_0(T_s,E_i,\theta_i)$ can be given by

$$S_0(T_s,E_i,\theta_i)=S_d^0(E_i,\theta_i)\exp[-E_{\rm dir}(E_i,\theta_i)/kT_s]+P_{\rm trap}(E_i,\theta_i)\{1+\nu_d/\nu_a\exp[-(E_d-E_a)/kT_s]\}^{-1}, \quad (2)$$

where $E_{\rm dir}(E_i,\theta_i)$, E_d, and E_a are activation energies for DC sticking the desorption, and the adsorption, respectively. The physisorption-mediated sticking has been well discussed in the context of the kinetic model, Eq. (2), by several groups,[1,6,9] who concluded that $E_d > E_a$ if $P_{\rm trap}$ is insensitive to T_s. But D'Evelyn *et al.*[9] did not agree with this assumption and disputed that such a decrease in S_0 with increasing T_s should be ascribed to $P_{\rm trap}$. However, $P_{\rm trap}$ were found to be rather insensitive to T_s above 300 K as mentioned above. Therefore, we still prefer the conventional kinetic process that the T_s dependence of sticking, which proceeds via physisorption, is mainly determined in the competitive process between sticking and desorption. The S_0 curve for $E_i=0.09$ eV in Fig. 2 can be best fitted to Eq. (2) for $E_d-E_a=21$ meV and $\nu_d/\nu_a=225$, assuming $S_0=0.01$ and $S_d^0=0$ (the solid line at $E_i=0.09$ eV in Fig. 2). Previously,[13] we also obtained similar results for E_d-E_a and ν_d/ν_a in the measurement of the O_2 desorption from the physisorption well, which can be considered as a competitive process to sticking.

The DC sticking at $E_i=0.9$ and 0.3 eV is promoted by a charge transfer from Si surfaces to the incident O_2 to form O_2^-. From the S_0 versus T_s curves in Fig. 2, we can estimate $E_{\rm dir}$ and S_d^0, which characterize this electron transfer in a collision of O_2 with Si surfaces. Using already evaluated values for E_d-E_a and ν_d/ν_a, and scaling S_0 with a value of 0.01 at 300 (Ref. 9) and $E_i=0.09$ eV, $E_{\rm dir}$ and S_d^0 at $E_i=0.9$ and 0.3 eV were estimated by means of a least-squares fit of the data in Fig. 2 to Eq. (2). The results are summarized in Table I. In order to facilitate the direct comparison of S_d between $E_i=0.9$ and 0.3 eV, the experimental values of S_d at 300 K are also tabulated. The solid lines for $E_i=0.9$ and 0.3 eV in Fig. 2 are the best fitted ones with the parameters given in Table I. S_d at $E_i=0.9$ eV is larger than that at $E_i=0.3$ eV by about a factor of 5. This increase in S_d with increasing E_i is found to be due to both terms of $\exp(-E_{\rm dir}/kT)$ and S_d^0. A Fermi distribution function instead of the Boltzmann distribution function for S_d gave almost the same values for $E_{\rm dir}$ to those in Table I.

TABLE I. Best-fitted parameters S_d^0 and $E_{\rm dir}$ at $E_i=0.9$ and 0.3 eV, and experimentally determined S_d at 300 K. For these parameters there exists a relation, $S_d=S_d^0\exp(-E_{\rm dir}/kT_s)$.

E_i (eV)	S_d^0	$E_{\rm dir}$ (meV)	S_d
0.9	0.028	23	0.0120
0.3	0.015	45	0.0026

The electron-transfer process from surfaces to incident O_2 may be adequately described with two-dimensional (Z,R) (Z, the position of O_2 with respect to the surface; and R, the internuclear distance between two oxygen atoms in O_2) potential-energy surfaces (PES), implicitly involving the orientation of O_2 and phonon coordinates. The importance of the implicit coordinates were particularly discussed by Luntz *et al.*[21] for O_2 sticking on Pt(111), where a temporary negative-ion state was also invoked for direct or quasidirect sticking. In order to understand the physical origin of $E_{\rm dir}$, schematic one-dimensional representation of the diabatic PES as a function of R are shown in Fig. 5. Measurable electron transfer is anticipated when the O_2^- potential curve crosses O_2+e^- potential curves at the region of zero-point vibrational level. If the O_2+e^- curve (curve 1) for the transferring electron at Fermi level is not the case of such curve crossing at the zero-point level, the O_2+e^- curve needs to be lifted to the upper energy region by $\Delta E_{1,2}$ to get crossing at the zero-point energy level (curve 2 or 3). $\Delta E_{1,2}$ are uniquely determined, once the relevant potential-energy curves are fixed. The most favorable curve crossing will occur at the bottom of the O_2+e^- curve for the highest probability amplitude of R for either the case of adiabatic[26] or diabatic transition.[25,27] The upward lifting of O_2+e^- may be performed by thermal activation of the transferring electron into the vacant surface states above the Fermi level. This potential crossing will vary with Z for different O_2 trajectories depending on E_i. When the incident O_2 has the larger E_i, it will approach the surface and then find the better configuration in PES for electron transfer to occur with much higher probability.[22] Then, ΔE_1 or ΔE_2 is dependent on E_i, and $\Delta E_1 < \Delta E_2$ is anticipated. The electron-

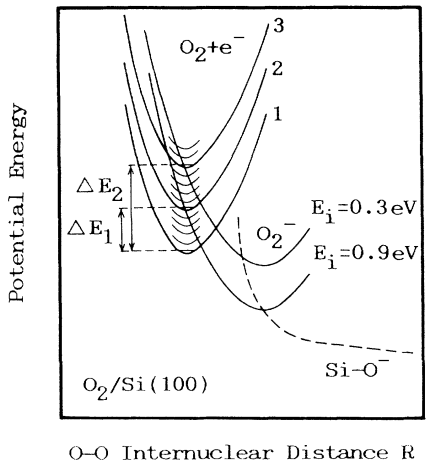

FIG. 5. Schematic one-dimensional representation of the diabatic PES for describing the electron transfer from the Si surface to the incident O_2. The diabatic PES is composed of three diabatic surfaces (from left to right) O_2+e^-, O_2^-, and Si-O^- (see text).

transfer probability can thus be proportional to the electron populations at the energy level of $\Delta E_{1,2}$ above E_F where two curves cross at the bottom of the O_2+e^- curve. Considering the continuous distribution of the surface density of states,[28] $D(E)$, the electron population at $E=E_F+\Delta E_{1,2}$ may be approximated in the form $D(E_F+\Delta E_{1,2})\exp(-\Delta E_{1,2}/kT_s)$ if $E_{\rm dir}$ is comparable to kT_s. Now, the physical origin of $E_{\rm dir}$ becomes clear, namely, $E_{\rm dir}$ is $\Delta E_{1,2}$ itself.

The essential point in the present argument is, therefore, very similar to the argument in the vibrational excitation of NO on Ag(111).[24] In the latter case, Rettner *et al.*[24] observed an activation energy of 0.23 eV, which is the vibrational energy of NO. This fact was considered as evidence for electron-transfer-induced vibrational excitation in the NO scattering at the surface. The activation energy $E_{\rm dir}$ for O_2 sticking at the Si surface is smaller by an order of magnitude than that for the vibrational excitation of NO. Such smaller $E_{\rm dir}$ predicts that the present electron transfer to O_2 from Si would be relevant to direct inelastic scattering from the O_2^- potential with no vibrational excitations of O_2, if it could be detected.

Rettner and Stein[29] observed a dramatic increase in S_0 with increasing E_i for dissociative adsorption of N_2 on Fe(111). It was found that S_0 also increased with decreasing T_s; a phenomenological activation energy of $E^*=-23$ meV was obtained at $E_i=1.05$ eV. This apparent negative activation energy was considered to exhibit a precursor to dissociation. The precursor model was reconciled with the observed activation of S_0 with E_i by invoking direct access to the intermediate state overcoming the distributed potential barriers. This scheme may invoke a rapid relaxation of the intermediate to its ground state. Our DC sticking scheme of O_2 on Si for high E_i, therefore, resembles Rettner and Stein's[29] scheme for N_2 sticking on Fe(111), because we also invoke the direct access to the intermediate O_2^- state followed by rapid relaxation to $O_2^-(a)$ as mentioned above. However, there is a clear difference in phenomenological activation energies between O_2/Si and N_2/Fe: The activation energy for dissociation of N_2 on Fe is apparently negative, while it is positive for O_2/Si. The phenomenological activation energy for sticking via direct access to molecularly chemisorbed intermediate state should be considered by dividing the process into two successive stages, the access to the intermediate state and the subsequent dissociation. Resonant dissociation in the latter process[30] might be possible, only when the process could be truly called "direct" sticking. Perhaps sticking of O_2 on Pt(111) (Reg. 21) and on W(110) (Ref. 31) may be the case. Once in a resonantly prepared O_2^- on Si, a rapid relaxation into $O_2^-(a)$ will lead to a finite lifetime, which may be determined by nuclear tunneling to dissociation even at such low T_s as 20 K,[1] while it may be limited by thermal activation to dissociation above 300 K. But if the surface is already oxidized to some extent, this barrier becomes so high that neither tunneling nor thermal activation occurs, and then some $O_2^-(a)$, whose formation may be also limited due to the reduced electron populations for the depletion of surface states by oxygen coverage, may be observable even at 300 K. In any case, since $O_2^-(a)$ eventually changes to Si-O^- definitely at high T_s and clean surface, the positive activation energy for sticking of O_2 on Si may mainly reflect the electron-transfer process.

In order to distinguish between the dissociation process and the temporary negative-ion state, the E_i dependence of both saturation coverage and yield of $O_2^-(a)$ at low T_s, and a dependence of those on surface states, i.e., whether *p* or *n* type, should be further investigated.

IV. SUMMARY

We have studied the dynamics of sticking and scattering of O_2 on Si(100) by using molecular-beam techniques. For $E_i=0.09$ eV, the scattering process is dominated by the trapping desorption. While for $E_i=0.9$ eV, it is dominated by direct inelastic scattering. The sticking or dissociative adsorption of O_2 showed quite different T_s dependences in low and high E_i corresponding to scattering measurements. For low E_i, a *decrease* in S_0 with increasing T_s is observed, while for high E_i, an *increase* in S_0 with increasing T_s is observed. The sticking process at low E_i was proposed to occur via physisorption followed by chemisorbed intermediate state of $O_2^-(a)$ from which sticking takes place. On the other hand, the sticking process at high E_i was discussed to occur via direct or resonant access to the O_2^- state.

ACKNOWLEDGMENTS

This work was supported by a Grant-in-Aid for Joint Research between University and Industry from the Japan Ministry of Education, Science and Culture.

[1]A. J. Schell-Sorokin and J. E. Demuth, Surf. Sci. **157**, 273 (1985).
[2]H. Ibach, H. D. Bruchmann, and W. Wagner, Appl. Phys. A **29**, 113 (1982).
[3]K. Edamoto, Y. Kubota, H. Kobayashi, M. Onchi, and M. Nishijima, J. Chem. Phys. **83**, 428 (1986).
[4]U. Höfer, P. Morgen, W. Wurth, and E. Umbach, Phys. Rev. Lett. **55**, 2927 (1985); U. Höfer, A. Puschmann, D. Coulman, and E. Umbach, Surf. Sci. **211/212**, 948 (1989).
[5]G. Hollinger and F. J. Himpsel, Phys. Rev. B **28**, 3651 (1983); G. Hollinger, J. F. Morar, F. J. Himpsel, G. Hughes, and J. L. Jordan, Surf. Sci. **168**, 609 (1986).
[6]P. Gupta, C. H. Mak, P. A. Coon, and S. M. George, Phys. Rev. B **40**, 39 (1989).
[7]C. Silvestre and M. Shayegan, Phys. Rev. B **37**, 10432 (1988).
[8]M. L. Yu and B. N. Eldridge, Phys. Rev. Lett. **58**, 1691 (1987).
[9]M. P. D'Evelyn, M. M. Nelson, and T. Engel, Surf. Sci. **186**, 75 (1987).
[10]J. R. Engstrom and T. Engel, Phys. Rev. B **41**, 1038 (1990).
[11]W. A. Goddard III, A. Redondo, and T. C. McGill, Solid State Commun. **18**, 981 (1976).
[12]For example, see review articles, J. A. Barker and D. J. Auerbach, Surf. Sci. Rep. **4**, 1 (1984); M. P. D'Evelyn and R. J. Madix, *ibid.* **3**, 413 (1983).
[13]T. Miyake, A. Namiki, T. Takemoto, S. Soeki, H. Kato, H. Kamba, T. Suzaki, and T. Nakamura, Jpn. J. Appl. Phys. **29**, 723 (1990).
[14]J. Eisinger and J. T. Law, J. Chem. Phys. **30**, 410 (1959); R. E. Schlier and H. E. Farnsworth, *ibid.* **30**, 917 (1959); R. J. Archer and G. W. Gobele, J. Phys. Chem. Solids **26**, 343 (1965); R. J. Madix and R. Korus, Trans. Faraday Soc. **64**, 2514 (1968); G. Rovida, E. Zanazzi, and E. Ferrone, Surf. Sci. **30**, 707 (1972); C. A. Carosella and J. Comas, *ibid.* **15**, 303 (1969); B. A. Joyce and J. H. Neave, *ibid.* **30**, 710 (1972); H. Ibach, K. Horn, R. Dorn, and H. Luth, *ibid.* **38**, 433 (1973); N. Kasupke and M. Henzler, *ibid.* **92**, 407 (1980); W. Ranke and Y. R. Xing, *ibid.* **157**, 353 (1985); P. Morgen, W. Wurth and E. Umbach, *ibid.* **152/153**, 1086 (1985).
[15]E. W. Kuipers, M. G. Tenner, M. E. M. Spruit, and A. W. Kleyn, Surf. Sci. **206**, 241 (1988).
[16]J. D. Levine, Surf. Sci. **34**, 90 (1973).
[17]E. M. Oellig, E. G. Michel, M. C. Asensio, and R. Miranda, Appl. Phys. Lett. **50**, 1660 (1987); E. M. Oellig and R. Miranda, Surf. Sci. Lett. **177**, 947 (1986).
[18]E. G. Michel, J. E. Ortega, E. M. Oellig, M. C. Acensio, J. Ferrón, and R. Miranda, Phys. Rev. B **38**, 13399 (1988).
[19]P. Soukiassian, T. M. Gentle, M. H. Bakshi, and Z. Hurych, J. Appl. Phys. **60**, 4339 (1986).
[20]J. H. Rechtien, U. Imke, K. J. Snowdon, P. H. F. Reijnen, P. J. van den Hoek, A. W. Kleyn, and A. Namiki, Nucl. Instrum. Methods B **48**, 339 (1990); Surf. Sci. **227**, 35 (1990).
[21]A. C. Luntz, M. D. Williams, and D. S. Bethune, J. Chem. Phys. **89**, 4381 (1988).
[22]M. E. M. Spruit, Ph.D. thesis, University of Amsterdam, 1988.
[23]P. Haochang, T. C. M. Horn, and A. W. Kleyn, Phys. Rev. Lett. **57**, 3035 (1986).
[24]C. T. Rettner, F. Fabre, J. Kimman, and D. J. Auerbach, Phys. Rev. Lett. **55**, 1904 (1985); C. T. Rettner, J. Kimman, F. Fabre, D. J. Auerbach, and H. Morawitz, Surf. Sci. **192**, 107 (1987).
[25]S. Holloway and J. W. Gadzuk, J. Chem. Phys. **82**, 5203 (1985); J. W. Gadzuk, *ibid.* **86**, 5196 (1987).
[26]D. Newns, Surf. Sci. **171**, 600 (1985).
[27]J. W. Gadzuk, Comments At. Mol. Phys. **16**, 219 (1985).
[28]S. M. Sze, *Physics of Semiconductor Devices* (Wiley, New York, 1981), p. 272.
[29]C. T. Rettner and H. Stein, Phys. Rev. Lett. **59**, 2768 (1987).
[30]J. W. Gadzuk and S. Holloway, Chem. Phys. Lett. **114**, 314 (1985).
[31]C. T. Rettner, L. A. DeLouise, and D. J. Auerbach, J. Chem. Phys. **85**, 1131 (1986).